

Schwinger-boson mean-field theory of the mixed-spin antiferromagnet $L_2\text{BaNiO}_5$

This article has been downloaded from IOPscience. Please scroll down to see the full text article.

2002 J. Phys.: Condens. Matter 14 8563

(<http://iopscience.iop.org/0953-8984/14/36/312>)

View [the table of contents for this issue](#), or go to the [journal homepage](#) for more

Download details:

IP Address: 171.66.16.96

The article was downloaded on 18/05/2010 at 14:57

Please note that [terms and conditions apply](#).

Schwinger-boson mean-field theory of the mixed-spin antiferromagnet $L_2\text{BaNiO}_5$

Yun Song and Shiping Feng

Department of Physics, Beijing Normal University, Beijing 100875, People's Republic of China

E-mail: yusong@bnu.edu.cn

Received 29 April 2002, in final form 10 July 2002

Published 29 August 2002

Online at stacks.iop.org/JPhysCM/14/8563

Abstract

The Schwinger-boson mean-field theory is used to study the three-dimensional antiferromagnetic (AF) ordering and excitations in the compounds $L_2\text{BaNiO}_5$, a large family of quasi-one-dimensional mixed-spin antiferromagnets. To investigate the magnetic properties of these compounds, we introduce a three-dimensional mixed-spin AF Heisenberg model based on experimental results for the crystal structure of $L_2\text{BaNiO}_5$. This model can explain the experimental finding of coexistence of the Haldane gap and AF long-range order below the Néel temperature. Properties such as the low-lying excitations, magnetizations of Ni and rare-earth ions, Néel temperatures of different compounds, and the behaviour of the Haldane gap below the Néel temperature are investigated within this model, and the results are in good agreement with neutron scattering experiments.

1. Introduction

The existence of a Haldane gap [1] in the magnetic excitation spectrum has maintained the integer-spin one-dimensional (1D) Heisenberg antiferromagnet as one of the most interesting subjects in condensed matter physics over the past 20 years. The integer-spin Heisenberg antiferromagnetic (AF) chain should have a singlet ground state, exponentially decaying correlations, and a quantum gap; these features have been confirmed by numerous theoretical [2–6] and experimental [7–10] studies. Kennedy and Tasaki have proved that the appearance of a Haldane gap in the spin-1 AF chain corresponds to the breaking of a hidden $Z_2 \times Z_2$ symmetry [11]. The recent finding of coexistence of the Haldane gap and AF long-range order (AF LRO) in the rare-earth compounds $L_2\text{BaNiO}_5$ with $L = \text{Y, Nd, Sm, Eu, Gd, Tb, Dy, Ho, Er, and Tm}$ [10, 12–16] has offered an opportunity to investigate the effect of a staggered field on the Haldane chain. Polarized and unpolarized inelastic neutron scattering experiments on $L_2\text{BaNiO}_5$ [14, 16] indicate, on the one hand, that there are AF interactions between spins of rare-earth and Ni ions, which lead to the three-dimensional (3D) AF LRO with the Néel temperature (T_N) ranging from 20 to 70 K [12, 13]; on the other hand, these

compounds are also characterized by the presence of NiO₆ octahedron chains along the *a*-axis. As was anticipated, above the Néel temperature, an energy gap has been found in the excitation propagating along the Ni chain. Also, the Haldane gap is discovered to persist in the 3D AF phase and increase with decreasing temperature below T_N [14–16].

Recently, several theoretical works have focused on the quasi-1D Haldane system L₂BaNiO₅ [17–19]. To describe the coexistence of the Haldane gap and AF LRO, the nonlinear sigma model for the scenario in a static staggered magnetic field has been introduced by Maslov and Zheludev [17]. This system has been studied numerically within the density matrix renormalization group method by adopting the model of a 1D spin-1 Heisenberg chain in a static field [18]. In the above studies, the reason for introducing the static staggered field is based on the assumption that there are 3D directly AF exchange interactions between the spins of rare-earth ions, which lead to the AF LRO below T_N . However, it has been pointed out on the basis of some experiments [12–14] that spins of Ni ions also play an important role in forming AF LRO, and the two-dimensional mixed-spin Heisenberg model with $s_1 = 1$ and $s_2 = 1/2$ chains stacked alternatively has also been adopted for this system [19].

In view of the experimental finding for the crystal structure, we introduce a more suitable 3D mixed-spin AF Heisenberg model to describe the magnetic properties of the compounds L₂BaNiO₅. In this model we define $s_1 = 1$ for the spins of Ni ions, and investigate different members of this family by changing the spin value s_2 of the rare-earth ions correspondingly. We use the Schwinger-boson mean-field (SBMF) [20–22] theory to study this 3D mixed-spin model. The SBF theory has been successful in the study of integer-spin Heisenberg chains [20, 21], and has also been extended to cases with magnetic ordering by identifying the magnetization with the Bose condensation of the Schwinger bosons [20–22]. Within this model, we can explain the experimental finding of the coexistence of the Haldane gap and AF LRO. The interactions between spins of Ni and rare-earth ions are proved to be very important in forming the AF LRO. Properties such as the magnetization, Haldane gap, and Néel temperatures are also discussed for cases with different s_2 . Comparing our results with neutron scattering experiments, we find that our findings could explain some experimental findings.

The paper is organized as follows. In section 2 we introduce the 3D mixed-spin Heisenberg model and SBF theory. Our results on the magnetic properties of L₂BaNiO₅ compounds are presented in section 3. Finally, we conclude our findings in section 4.

2. The mixed-spin Heisenberg model and Schwinger-boson mean-field theory

The crystal structures of L₂BaNiO₅ compounds have been investigated extensively by means of neutron scattering experiments [12–14]. They belong to the orthorhombic system, having approximate cell parameters around $a = 3.8 \text{ \AA}$, $b = 5.8 \text{ \AA}$, and $c = 11.3 \text{ \AA}$. In all members of this compound group, as figure 1(b) shows, strings of distorted NiO₆ octahedra share the apical oxygen and form Haldane chains along the *a*-axis. The intrachain Ni–O–Ni AF superexchange coupling is about 200–300 K [12–14], which is the strongest magnetic interaction in the compound. However, in the *bc*-plane, as figure 1(a) shows, there is one oxygen between the Ni and rare-earth (L) ions, and thus the Ni–O–L interactions establish links between individual Ni chains. This coupling is of the order of tens of kelvins (10–30 K). Figure 1(a) also shows that there are L–O–L AF interactions between rare-earth ions, which are of the order of 1 K or less.

On the basis of the experimental finding of the crystal structure of the compounds L₂BaNiO₅, we introduce a 3D mixed-spin AF Heisenberg model expressed by the Hamiltonian

$$H = J_1 \sum_{i, \eta_a} S_{1,i} S_{1,i+\eta_a} + J_2 \sum_{i, \eta_b, \eta_c} S_{1,i} S_{2,i+\eta_b+\eta_c} + J_3 \sum_j S_{2,j} S_{2,j+\hat{c}_0}, \quad (1)$$

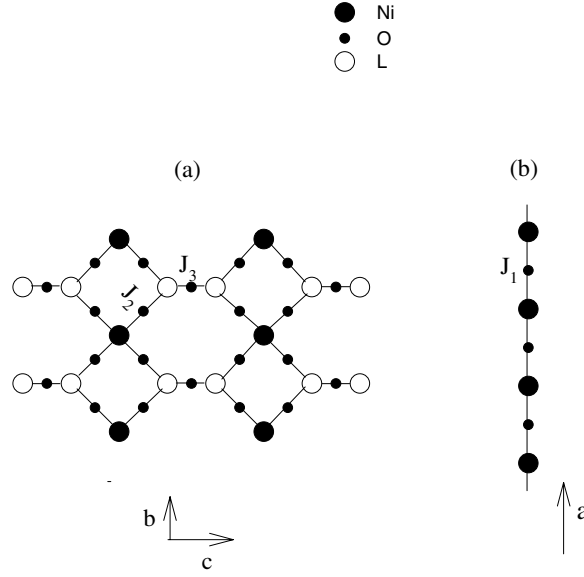


Figure 1. (a) Structural relation between Ni and rare-earth sites in the bc -plane, and (b) Ni and apical oxygen form the Haldane chain along the a -axis.

where S_1 and S_2 are the spin operators of the Ni and rare-earth ions respectively. η_b and η_c denote summations over nearest-neighbour (NN) bonds in the bc -plane, and η_a that over the NN bonds along the a -axis. The AF superexchange couplings along the Ni chain, between L and Ni ions, and among the rare-earth L ions are represented as J_1 , J_2 , and J_3 respectively, as figure 1(a) shows.

The Schwinger-boson theory introduces $S_i = \frac{1}{2}b_{i\alpha}^+ \sigma_{\alpha\beta} b_{i\beta}$ (α (or β) = \uparrow, \downarrow) [20, 21], and the spin degrees of freedom are mapped to the boson degrees of freedom. Meanwhile, the original spin Hilbert space corresponds to a boson Hilbert subspace in which $b_{i\uparrow}^+ b_{i\uparrow} + b_{i\downarrow}^+ b_{i\downarrow} = 2s_i$. These constraints on the boson Hilbert space are imposed in the Hamiltonian (1) by introducing two kinds of Lagrangian multiplier, $\lambda_1(i)$ and $\lambda_2(j)$. In addition, we define the bond operators as $Q_a(i, \eta_a) = b_{1i\uparrow} b_{1(i+\eta_a)\downarrow} - b_{1i\downarrow} b_{1(i+\eta_a)\uparrow}$, $Q_h(i, \eta_b, \eta_c) = b_{1i\uparrow} b_{2(i+\eta_b+\eta_c)\downarrow} - b_{1i\downarrow} b_{2(i+\eta_b+\eta_c)\uparrow}$, and $Q_c(j, \hat{c}_0) = b_{2j\uparrow} b_{2(j+\hat{c}_0)\downarrow} - b_{2j\downarrow} b_{2(j+\hat{c}_0)\uparrow}$. The Hamiltonian (1) can be rewritten as

$$\begin{aligned}
 H = & -\frac{1}{2}J_1 \sum_{i, \eta_a} \{Q_a^+(i, \eta_a) Q_a(i, \eta_a) - 2s_1^2\} - \frac{1}{2}J_3 \sum_j \{Q_c^+(j, \hat{c}_0) Q_c(j, \hat{c}_0) - 2s_2^2\} \\
 & - \frac{1}{2}J_2 \sum_{i, \eta_b, \eta_c} \{Q_h^+(i, \eta_b, \eta_c) Q_h(i, \eta_b, \eta_c) - 2s_1 s_2\} \\
 & + \sum_i \lambda_1(i) \{b_{1i\uparrow}^+ b_{1i\uparrow} + b_{1i\downarrow}^+ b_{1i\downarrow} - 2s_1\} \\
 & + \sum_j \lambda_2(j) \{b_{2j\uparrow}^+ b_{2j\uparrow} + b_{2j\downarrow}^+ b_{2j\downarrow} - 2s_2\}. \tag{2}
 \end{aligned}$$

Next, we make a Hartree–Fock decomposition of equation (2) by taking the average values of the bond operators and Lagrange multipliers to be uniform and static: $\langle Q_a(i, \eta_a) \rangle = Q_a$, $\langle Q_h(i, \eta_b, \eta_c) \rangle = Q_h$, $\langle Q_c(j, \hat{c}_0) \rangle = Q_c$, $\langle \lambda_1(i) \rangle = \lambda_1$, and $\langle \lambda_2(j) \rangle = \lambda_2$. Under Fourier

transformation, we obtain the following mean-field Hamiltonian in the momentum space:

$$\begin{aligned}
H^{MF} = & \sum_k 2Z_k \{b_{1k\uparrow} b_{1(-k)\downarrow} - b_{1k\downarrow} b_{1(-k)\uparrow} + \text{h.c.}\} \\
& + \sum_k 4D_k \{b_{1k\uparrow} b_{2(-k)\downarrow} - b_{1k\downarrow} b_{2(-k)\uparrow} + \text{h.c.}\} \\
& + \sum_k 2\chi_k \{b_{2k\uparrow} b_{2(-k)\downarrow} - b_{2k\downarrow} b_{2(-k)\uparrow} + \text{h.c.}\} \\
& + \sum_{k\sigma} \{4\lambda_1 b_{1k\sigma}^+ b_{1k\sigma} + 8\lambda_2 b_{2k\sigma}^+ b_{2k\sigma}\} + 2N\{J_1 Q_a^2 + 4J_2 Q_h^2 \\
& + J_3 Q_c^2 - 4\lambda_1 s_1 + 2J_1 s_1^2 + 8J_2 s_1 s_2 + 2J_3 s_2^2 - 8\lambda_2 s_2\}, \tag{3}
\end{aligned}$$

where $Z_k = J_1 Q_a \cos(k_x a_0)$, $\chi_k = J_3 Q_c \cos(k_x c_0)$, and $D_k = 2J_2 Q_h \cos(k_x c_0) \cos(k_y b_0)$.

Diagonalizing H^{MF} in equation (3) by the Bogoliubov transformation, we obtain

$$H^{MF} = 2 \sum_k \{E_k^+ (\alpha_{1k\sigma}^+ \alpha_{1k\sigma} + \alpha_{2k\sigma} \alpha_{2k\sigma}^+) + E_k^- (\beta_{1k\sigma}^+ \beta_{1k\sigma} + \beta_{2k\sigma} \beta_{2k\sigma}^+)\} + E_0 \tag{4}$$

with

$$\begin{aligned}
E_k^\pm &= \sqrt{\frac{A \pm \sqrt{A^2 - 4B}}{2}} \\
A &= \lambda_1^2 + 4\lambda_2^2 - (Z_k^2 + \chi_k^2 + 2D_k^2) \\
B &= 4\lambda_1 \lambda_2 (\lambda_1 \lambda_2 - D_k^2) - \chi_k^2 \lambda_1^2 - 4Z_k^2 \lambda_2^2 + (\chi_k Z_k - D_k^2)^2 \\
E_0 &= 2N\{J_1 Q_a^2 + 4J_2 Q_h^2 + J_3 Q_c^2 + 2J_1 s_1^2 + 8J_2 s_1 s_2 + 2J_3 s_2^2\} \\
&\quad - 8N\lambda_1 (s_1 + \frac{1}{2}) - 16N\lambda_2 (s_2 + \frac{1}{2}). \tag{5}
\end{aligned}$$

Furthermore, the mean-field free energy is given by

$$F^{MF} = \frac{8}{\beta} \sum_k \ln \left\{ \left(2 \sinh \left(\frac{\beta E_k^+}{2} \right) \right) + \ln \left(2 \sinh \left(\frac{\beta E_k^-}{2} \right) \right) \right\} + E_0. \tag{6}$$

The mean-field equations are obtained by differentiating F^{MF} with respect to the parameters Q_a , Q_h , Q_c , λ_1 and λ_2 :

$$\frac{\partial F^{MF}}{\partial Q_a} = \frac{\partial F^{MF}}{\partial Q_h} = \frac{\partial F^{MF}}{\partial Q_c} = \frac{\partial F^{MF}}{\partial \lambda_1} = \frac{\partial F^{MF}}{\partial \lambda_2} = 0. \tag{7}$$

Thus we obtain five self-consistent equations to determine the average values of the bond operators and Lagrange multipliers.

3. Mean-field solutions

In this section, we present the solutions of the SBMF theory. The experimental finding of the coexistence of the Haldane gap and AF LRO below T_N is obtained in our study. As equation (5) shows, there are two branches of the magnetic excitations, E_k^+ and E_k^- , which have quite different behaviours below T_N . On the one hand, the magnetic excitation E_k^+ has an energy gap over the whole temperature region and below T_N this energy gap increases with decreasing temperature. On the other hand, within the temperature region from zero to T_N , E_k^- remains gapless and has its minimal value $E_k^- = 0$ at $k = 0$. Under this condition, the Schwinger-boson condensation occurs and leads to the AF LRO in this system. In our

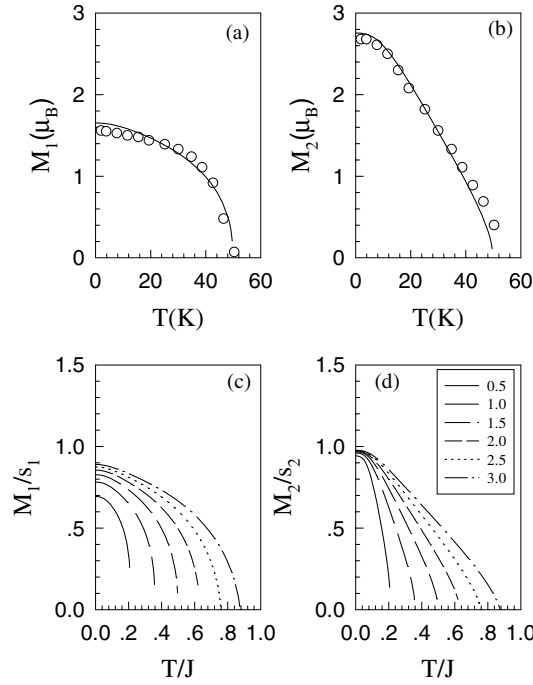


Figure 2. The temperature dependence of the ordered moment on the Ni (a) and Nd (b) sites in a $\text{Nd}_2\text{BaNiO}_5$ sample taken from [14] (open circles); the solid curves show fits to the experimental finding, from our numerical results, of the case with $s = 3/2$. Magnetizations M_1/s_1 (c) and M_2/s_2 (d) are shown as functions of temperature below T_N for the cases of $s_2 = 1/2, 1, 3/2, 2, 5/2$ and 3.

calculation, we introduce the Schwinger-boson condensation into the self-consistent mean-field equations, and obtain the temperature dependence of the magnetizations of Ni (M_1) and rare-earth (M_2) ions below T_N respectively. The magnetizations M_1 and M_2 are expressed as

$$M_1 = \langle S_1^Z \rangle = \frac{1}{2N} \sum_i \langle b_{1i\uparrow}^+ b_{1i\uparrow} - b_{1i\downarrow}^+ b_{1i\downarrow} \rangle$$

$$M_2 = \langle S_2^Z \rangle = \frac{1}{2N} \sum_j \langle b_{2j\uparrow}^+ b_{2j\uparrow} - b_{2j\downarrow}^+ b_{2j\downarrow} \rangle. \quad (8)$$

We choose the AF superexchange interactions as $J_1 = J$, $J_2 = 0.1J$ and $J_3 = 0.01J$ ($J > 0$) according to the experimental studies of the magnetic properties of the compounds $L_2\text{BaNiO}_5$ [12–14]. The AF interactions between Ni ions have been estimated as $2J = 200$ – 300 K from the neutron scattering experiments [12, 14]. For simplicity and clarity, in our calculations we choose $J = 100$ K.

The neutron scattering experimental results on $\text{Nd}_2\text{BaNiO}_5$ obtained by Yokoo *et al* [15] are shown in figures 2(a) and (b) (open circles). The solid curves in figures 2(a) and (b) show fits to the above experimental results of our numerical calculations for the case with $s_2 = 3/2$. The temperature dependences of magnetizations M_1/s_1 and M_2/s_2 for the cases of $s_2 = 1/2, 1, 3/2, 2, 5/2$ and 3 are shown in figures 2(c) and (d) respectively. As temperature increases, the thermal fluctuation in the system becomes stronger, and the magnetizations decrease rapidly and drop to zero at the Néel temperatures. Therefore, we could also determine the Néel temperatures T_N for all members of the $L_2\text{BaNiO}_5$ family through our calculation.

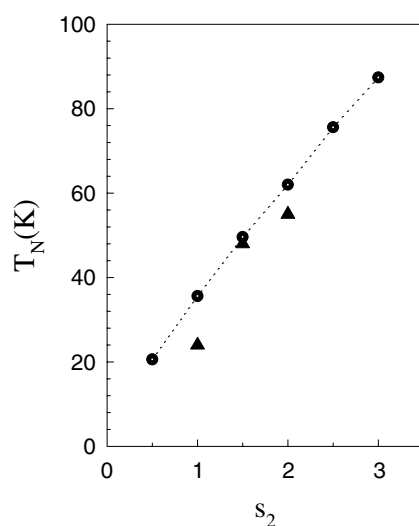


Figure 3. Néel temperatures of the compounds $L_2\text{BaNiO}_5$ for cases with different spin values s_2 . The circles represent the theoretical results and the triangles are experimental findings for the compounds $\text{Nd}_2\text{BaNiO}_5$, $\text{Pr}_2\text{BaNiO}_5$ and $\text{Ho}_2\text{BaNiO}_5$ taken from [11–13].

In figure 3, we plot the Néel temperature T_N as a function of spin value s_2 (filled circles and dotted curve). For comparison, the Néel temperatures of the compounds $\text{Ho}_2\text{BaNiO}_5$ ($T_N = 53$ K) [12], $\text{Nd}_2\text{BaNiO}_5$ ($T_N = 48$ K) [13] and $\text{Pr}_2\text{BaNiO}_5$ ($T_N = 24$ K) [14] obtained by neutron scattering experiments are also shown in figure 3 (filled triangles). Our theoretical results roughly agree with the experimental results. We also find that the Néel temperature T_N increases monotonically with increasing of s_2 . When the spin value of the rare-earth ions s_2 is equal to $1/2$ and 3 , we get that the minimum and maximum Néel temperatures are $T_N^{\min} \approx 0.207J$ and $T_N^{\max} \approx 0.872J$ respectively. Our result for the Néel temperature region is approximately from 20.7 to 87.2 K when $J = 100$ K, which is in good agreement with the experimental estimate of the T_N -region: 20–70 K [12, 13].

The two branches of the magnetic excitation, E_k^+ and E_k^- , represent the spin fluctuations along the a -axis and within the bc -plane respectively. In the exactly one-dimensional case ($J_2 = J_3 = 0$), the excitation E_k^- vanishes and the energy gap of E_k^+ is just the Haldane gap of the AF Heisenberg chain, which is closely related to the breaking of a hidden $Z_2 \times Z_2$ symmetry [11]. We obtain that the coexistence of the Haldane gap and AF LRO below T_N is a common feature of all compounds $L_2\text{BaNiO}_5$ except Y_2BaNiO_5 . The neutron scattering experiments have found that, below the Néel temperature, the Haldane gap increases as the temperature decreases [14–16]. The temperature dependences of the Haldane gap Δ for the cases of $s_2 = 1/2, 1, 3/2, 2, 5/2$ and 3 are also investigated by the SBMF theory and the behaviours are shown in figure 4(a). The temperature dependence of the energy gap Δ obtained by our calculation is found to agree with the experimental finding.

Our calculation also implies that the effect of the staggered magnetization on the magnetic excitation is to widen the Haldane gap. Below T_N , the effective internal magnetic field H_{eff} imposed on the Haldane chain is assumed approximately as the magnetization M_1 of Ni ions. This field is found to increase with decreasing temperature and increasing spin value s_2 because of the thermal fluctuation being weakened and the AF ordering being enhanced. In figure 4(b), we plot the energy gap Δ of zero temperature as a function of H_{eff} , and we find that H_{eff} has strong effect of widening the Haldane gap.

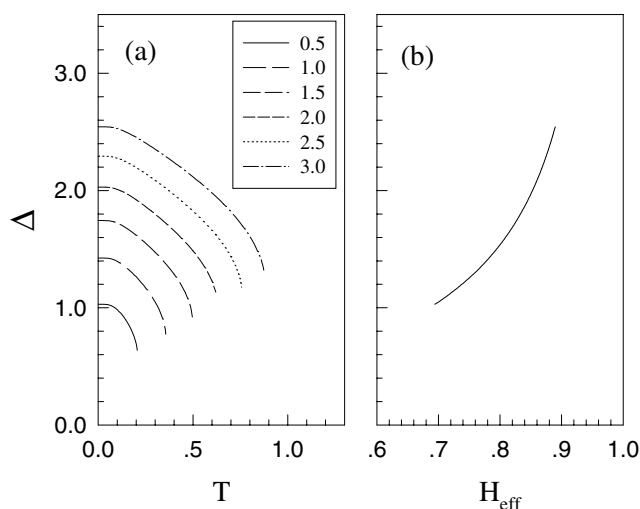


Figure 4. The temperature dependence of the Haldane gap for the cases of $s_2 = 1/2, 1, 3/2, 2, 5/2$ and 3 below the Néel temperatures; (b) the Haldane gap as a function of the effective internal magnetic field H_{eff} .

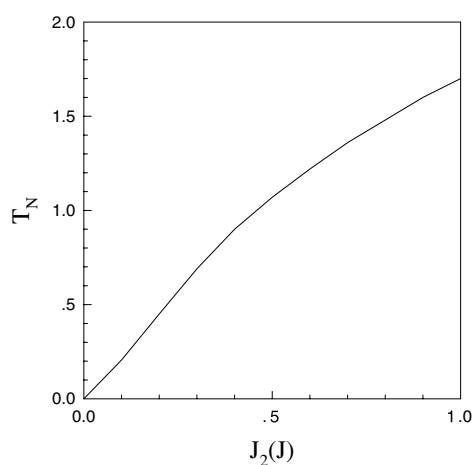


Figure 5. Néel temperature as a function of AF coupling J_2 between Ni^{2+} and L^{3+} ions for the case $s_2 = 1/2, J_1 = J, J_3 = 0.01J$.

In addition, on the basis of the 3D mixed-spin model, we obtain that AF LRO below the Néel temperature is not constructed only by the rare-earth ions. Our results support the suggestion that Ni ions also play an important role in forming the AF LRO. We plot in figure 5 the Néel temperature as a function of the AF coupling J_2 in the cases with $s_2 = 1/2, J_1 = J$ and $J_3 = 0.01J$. In the compounds $L_2\text{BaNiO}_5$, the effective interactions between individual Ni chains rely on the AF coupling J_2 between Ni^{2+} and rare-earth L^{3+} . We obtain that the Néel temperature rises rapidly with increase of J_2 as shown in figure 5, so the coupling J_2 is important in forming the AF LRO. Also, as $J_2 = 0$, there are no interactions between Ni chains and thus the Néel temperature drops to zero. The Haldane excitation energies E_k^+ in the 3D and 1D cases are shown in figures 6(a) and (b) respectively. Here we choose $s_2 = 1/2$,

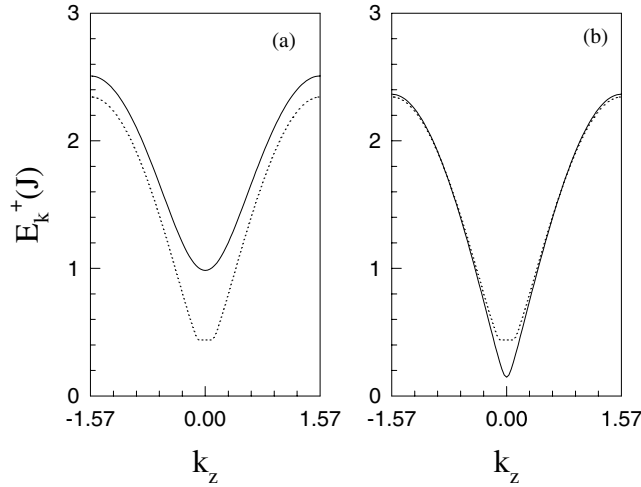


Figure 6. The branch of the Haldane excitation E_k^+ as a function of k_z in (a) 3D with $s_2 = 1/2$, $J_1 = J$, $J_3 = 0.01J$ and (b) the pure 1D case. The solid curves show results for temperature $T = 0.1J$ and the dotted curves present results for $T = 0.4J$.

$J_1 = J$, $J_2 = 0.01J$, $J_3 = 0.01J$ and $k_x = k_y = 0$ for the 3D case and obtain that the corresponding Néel temperature is $T_N = 0.206J$. To compare the behaviours of magnetic excitations below and above the Néel temperature, we study two conditions: $T = 0.1$ (solid curves) and $T = 0.4J$ (dotted curves) for both 1D and 3D cases. In the 3D case, we find, in figure 6(a), that the energy gap below the Néel temperature is obviously bigger than that above the Néel temperature, which is opposite to the behaviour for the pure 1D case (shown in figure 6(b)). In addition, we obtain that the thermal fluctuation has a strong effect of destroying the 3D spin correlations in the compounds; as a result, the behaviour in the 3D case is the same as that in the 1D case when the temperature is above the Néel temperature.

4. Summary

In conclusion, we have introduced a 3D mixed-spin AF Heisenberg model based on the experimental results for the crystal magnetic structure for the compounds $L_2\text{BaNiO}_5$, and studied this model with the SBMF theory. The experimental finding of coexistence of the Haldane gap and AF LRO below T_N has been deduced by our calculation. Properties such as the low-lying excitations, magnetizations of Ni and rare-earth ions, Néel temperatures of different members of this family and behaviour of the Haldane gap below T_N have also been investigated within this model.

We have obtained two branches of the magnetic excitations E_k^+ and E_k^- ; E_k^+ has an energy gap and E_k^- is gapless below T_N . The theoretical result is that the Néel temperature region is approximately from 20.7 to 87.2 K, which is in good agreement with the experimental estimate of the region: 20–70 K. We have also found that the Haldane gap increases with decreasing temperature, and the effect of the magnetization is to widen the Haldane gap. Our results are in good agreement with the experimental findings. Our findings also support the suggestion that the AF LRO below T_N is not constructed just by the rare-earth ions; Ni ions also play an important role in forming the AF LRO.

Acknowledgments

We thank Dr Xintian Wu for helpful discussions. This work was supported by the National Natural Science Foundation of China under Grant Nos 10125415, 10074007 and 90103024.

References

- [1] Haldane F D M 1983 *Phys. Lett. A* **93** 464
Haldane F D M 1983 *Phys. Rev. Lett.* **50** 1153
- [2] Affleck I 1989 *J. Phys.: Condens. Matter* **1** 3047
- [3] Nightingale M P and Blöte H W J 1986 *Phys. Rev. B* **33** 619
- [4] Nomura K 1989 *Phys. Rev. B* **40** 2421
- [5] Sakai T and Takahashi M 1990 *Phys. Rev. B* **42** 1090
- [6] Meshkov S V 1993 *Phys. Rev. B* **48** 6167
- [7] Morra R M, Buyers W J L, Armstrong R L and Hirakawa K 1988 *Phys. Rev. B* **38** 543
- [8] Ma S, Broholm C, Reich D H, Sternlieb B J and Erwin R W 1992 *Phys. Rev. Lett.* **69** 3571
- [9] Zheludev A, Nagler S E, Shapiro S M, Chou L K, Talham D R and Meisel M W 1996 *Phys. Rev. B* **53** 15 004
- [10] Buttrey D J, Sullivan J D and Rheingold A L 1990 *J. Solid State Chem.* **88** 291
- [11] Kennedy T and Tasaki H 1992 *Phys. Rev. B* **45** 304
Kennedy T and Tasaki H 1994 *Rev. Math. Phys.* **6** 887
- [12] García-Matres E, Rodríguez-Carvajal J, Martínez J L, Salinas-Sánchez A and Sáez-Puche R 1993 *Solid State Commun.* **85** 553
- [13] Sachan V, Buttrey D J, Tranquada J M and Shirane G 1994 *Phys. Rev. B* **49** 9658
- [14] Zheludev A, Tranquada J M, Vogt T and Buttrey D J 1996 *Phys. Rev. B* **54** 6437
- [15] Yokoo T *et al* 1998 *Phys. Rev. B* **58** 14 424
- [16] Raymond S, Yokoo T, Zheludev A, Nagler S E, Wildes A and Akimitsu J 1999 *Phys. Rev. Lett.* **82** 2382
- [17] Maslov S and Zheludev A 1998 *Phys. Rev. B* **57** 68
Maslov S and Zheludev A 1998 *Phys. Rev. Lett.* **80** 5786
- [18] Lou J, Dai X, Qin S, Su Z and Yu L 1999 *Phys. Rev. B* **60** 52
- [19] Takushima Y, Koga A and Kavakain N 2000 *Phys. Rev. B* **61** 15 189
- [20] Arovas D P and Auerbach A 1988 *Phys. Rev. B* **38** 316
Yoshioka D 1989 *J. Phys. Soc. Japan* **58** 32
- [21] Auerbach A 1994 *Interacting Electrons and Quantum Magnetism* (New York: Springer)
- [22] Sarker S, Jayaprakash C, Krishnamurthy H R and Ma M 1989 *Phys. Rev. B* **40** 5028
Kane C L, Lee P A, Ng T K, Chakraborty B and Read N 1990 *Phys. Rev. B* **41** 2653